Electronic Supplementary Material (ESI) for Inorganic Chemistry Frontiers.

Bioorthogonal Time-Resolved Luminogenic Probe for Metabolic Labelling and Imaging of Glycans

Judun Zheng,[d] Qiuqiang Zhan,[c] Lijun Jiang,[b] Da Xing,*[a] Tao Zhang,*[a] and Ka-Leung Wong*[b]

[a.] MOE Key Laboratory of Laser Life Science & Institute of Laser Life Science, Guangdong Provincial Key Laboratory of Laser Life Science, College of Biophotonics, South China Normal University, Guangzhou 510631, P. R. China.

[b.] Department of Chemistry, Hong Kong Baptist University, Kowloon Tong, Hong Kong SAR, P.R. China.

[c.] Centre for Optical and Electromagnetic Research, South China Academy of Advanced Optoelectronics, South China Normal University, Guangzhou, 510006, P.R. China.

[d.] Dermatology Hospital, Southern Medical University, Guangzhou 510091, P. R. China.

Catalogue

Experimental Procedures

Synthesis of the Tb-M. The general procedure syntheses of Tb-M is the same as the synthesis of Tb-1.

Compound 3. ^{1}H NMR (400 MHz, d_6-DMSO): δ 11.22 (s, 1H), 8.08 (d, *J* = 3.0 Hz, 1H), 6.13 (s, 2H), 5.74 (s, 1H), 5.41 (t, *J* = 3.0 Hz, 2H), 5.20 (d, *J* = 3.0 Hz, 2H), 5.18 (d, *J* = 3.0 Hz, 1H), 3.97 – 4.19 (m, 7H), 2.16 (s, *J* = 3.0 Hz, 1H), 2.03 (m, 25H), 1.91 (s, *J* = 3.0 Hz, 1H). ESI-MS (m/z): calcd for $C_{19}H_{19}N_3O_2$, 321.37 [M]; found, 320.8000.

Compound 4. ESI-MS (m/z): calcd for $C_{33}H_{40}N_6O_{11}$, 696.70 [M]; found, 696.4000.

Tb-M. ESI-MS (m/z): calcd for $C_{33}H_{36}N_6O_{11}Tb^{3+}$, 851.60 [M]; found, 851.1000.

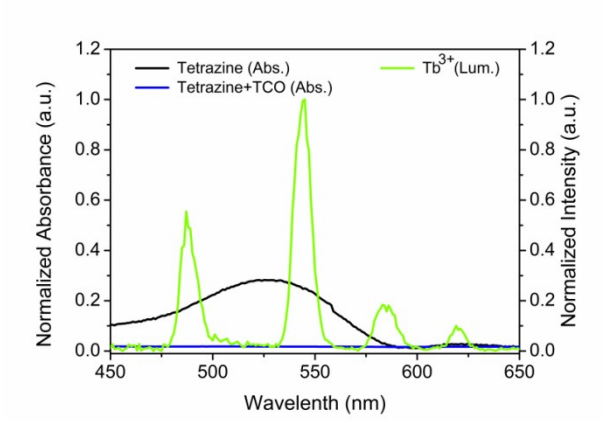

Fig. S1. Absorbance spectra (Abs.) of tetrazine in the absence or presence of TCO (black and blue line), together with the luminescence emission spectrum (Lum., green line) of Tb^{3+}, λ_{ex} = 340 nm.

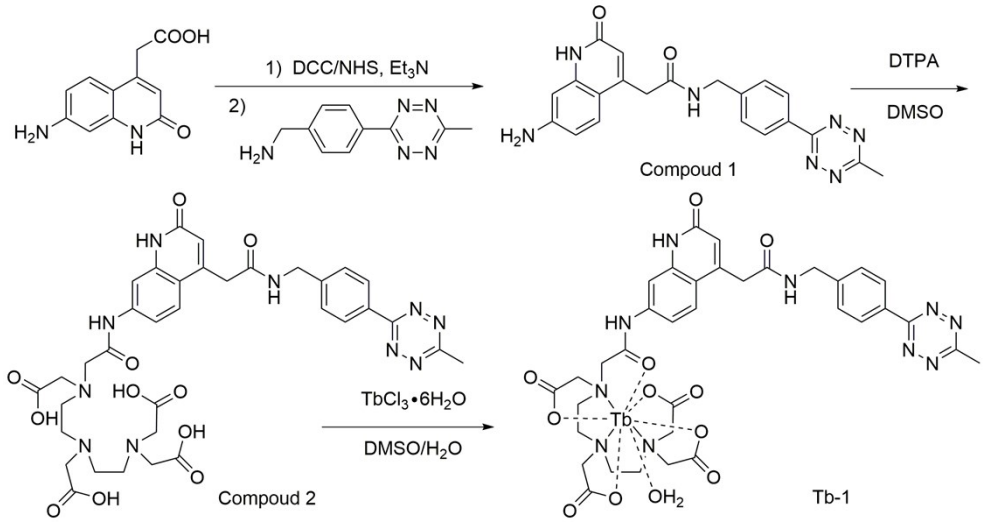

Fig. S2. Synthetic route of Tb-1.

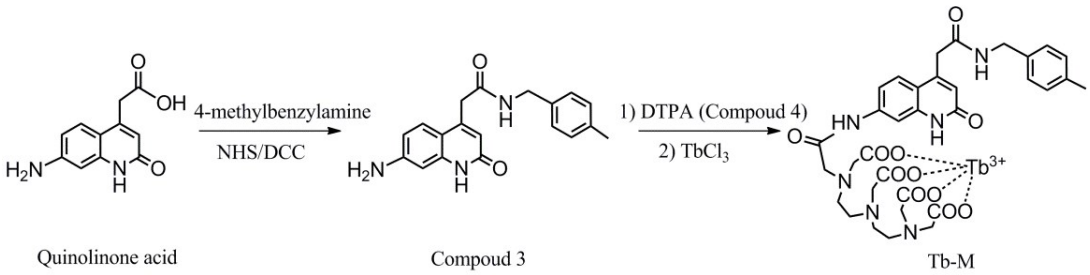

Fig. S3. Synthetic route of Tb-M.

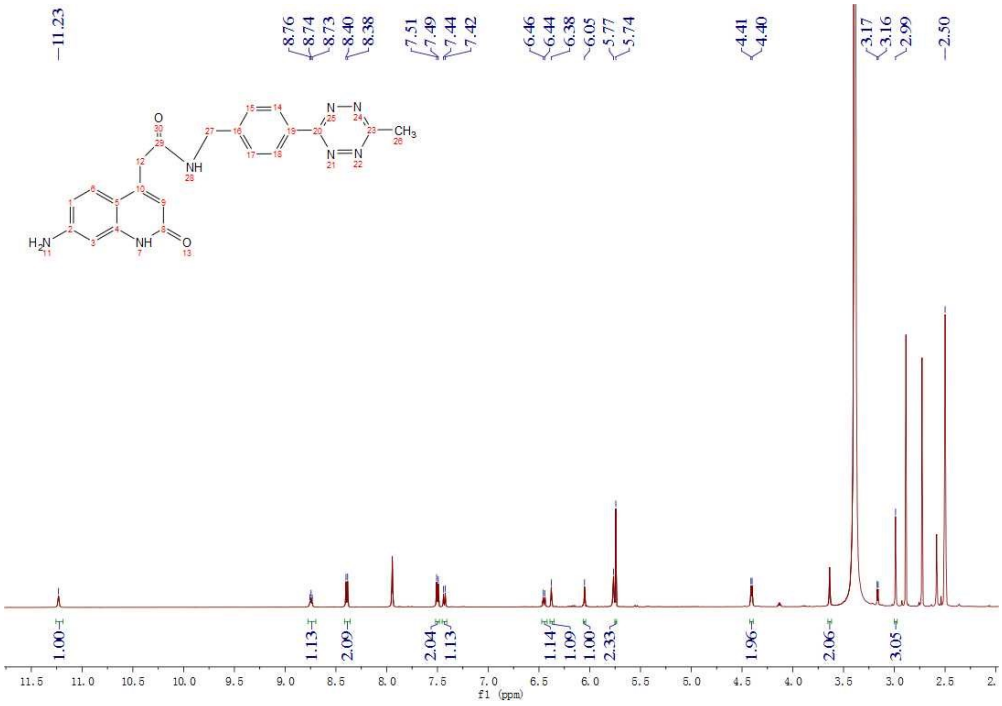

Fig. S4. ^{1}H NMR (400 MHz, d_6-DMSO) spectrum of compound 1.

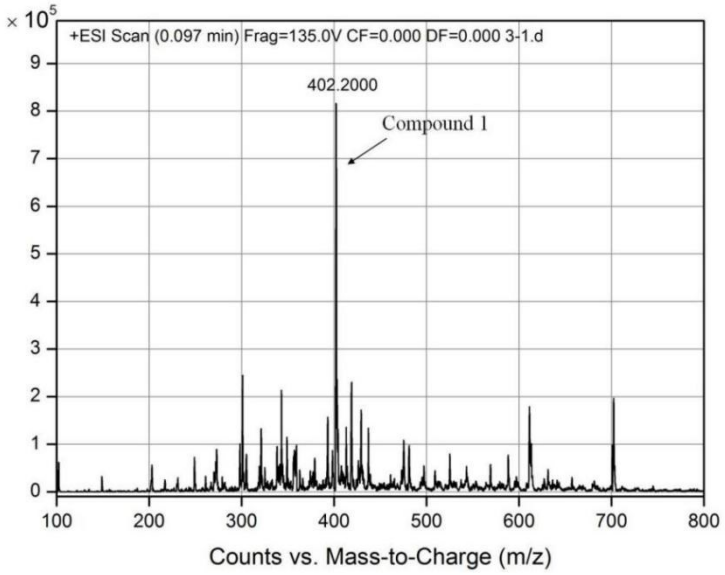

Fig. S5. ESI-MS spectrum of compound 1.

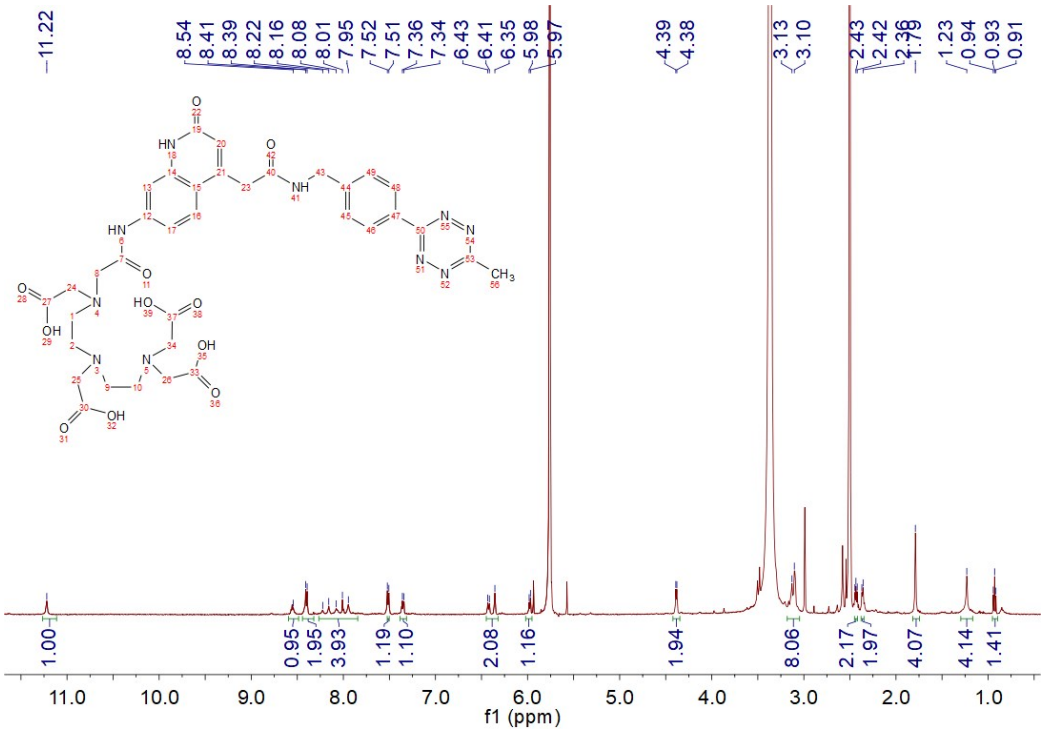

Fig. S6. ^{1}H NMR (400 MHz, d_6-DMSO) spectrum of compound 2.

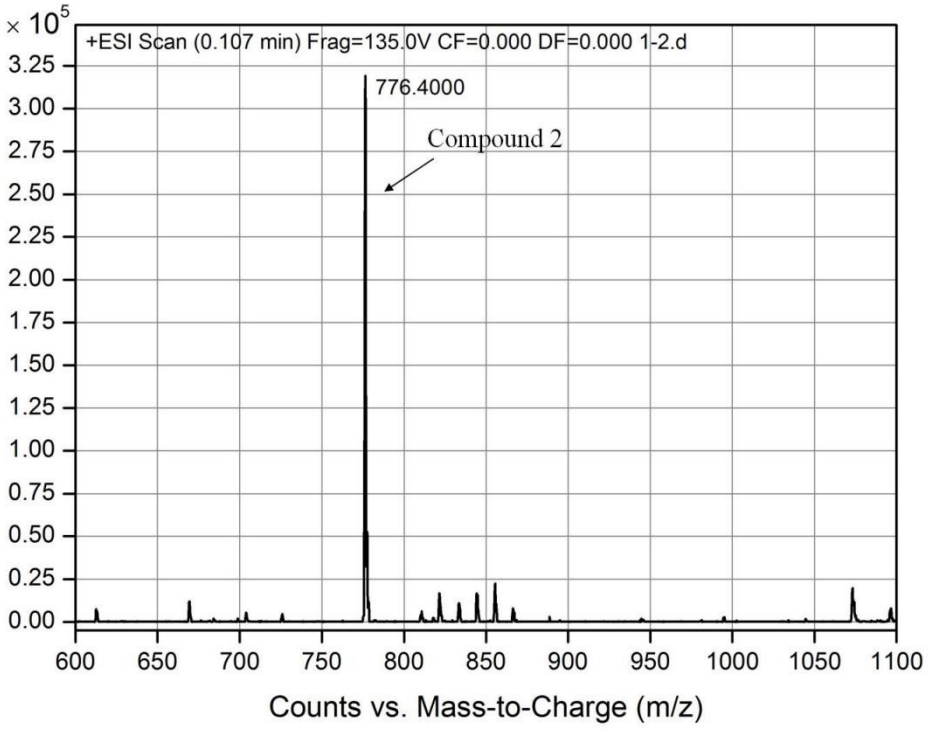

Fig. S7. ESI-MS spectrum of compound 2.

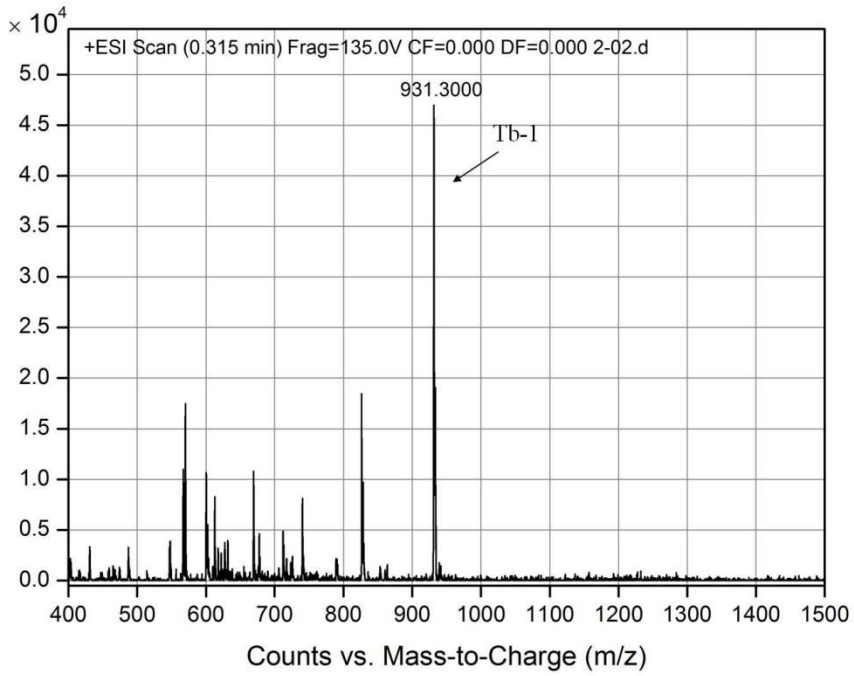

Fig. S8. ESI-MS spectrum of Tb-1.

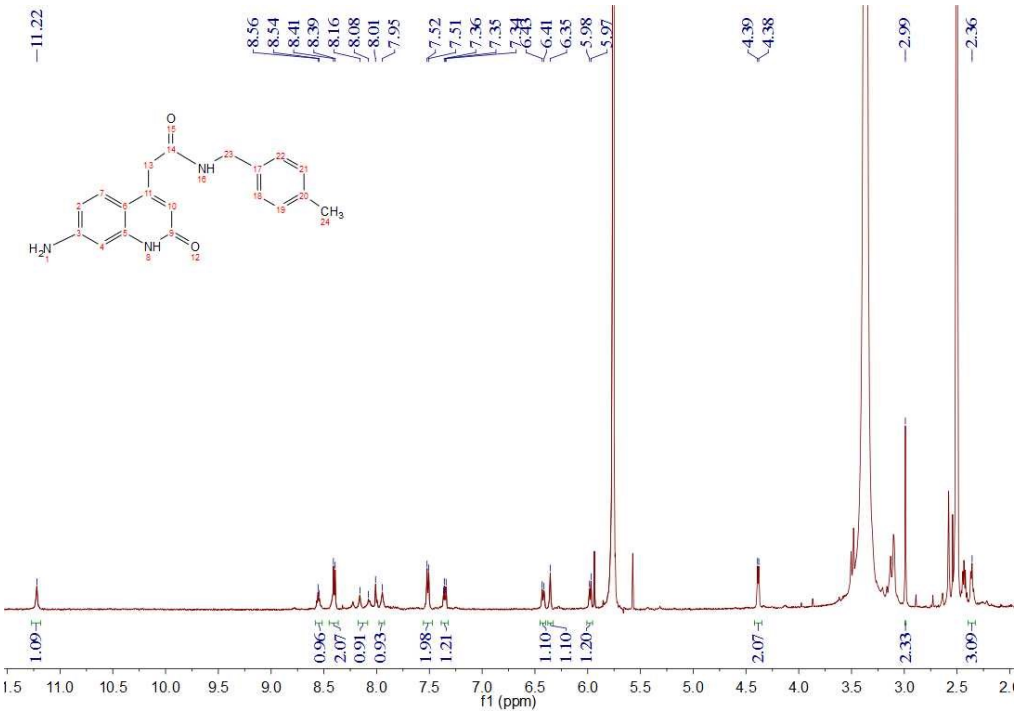

Fig. S9. ^{1}H NMR (400 MHz, d_6-DMSO) spectrum of compound 3.

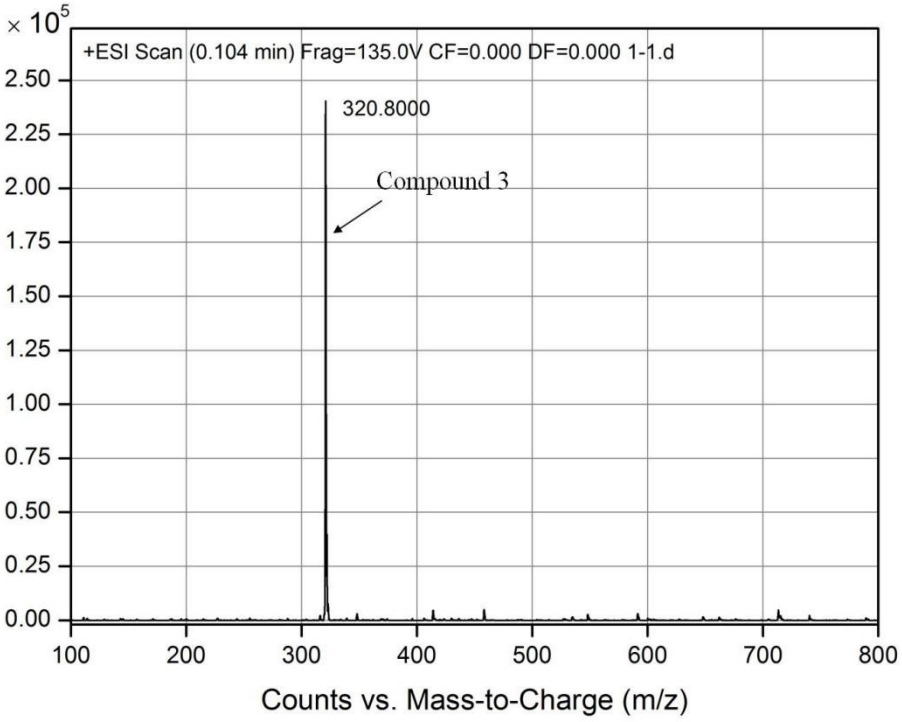

Fig. S10. ESI-MS spectrum of compound 3.

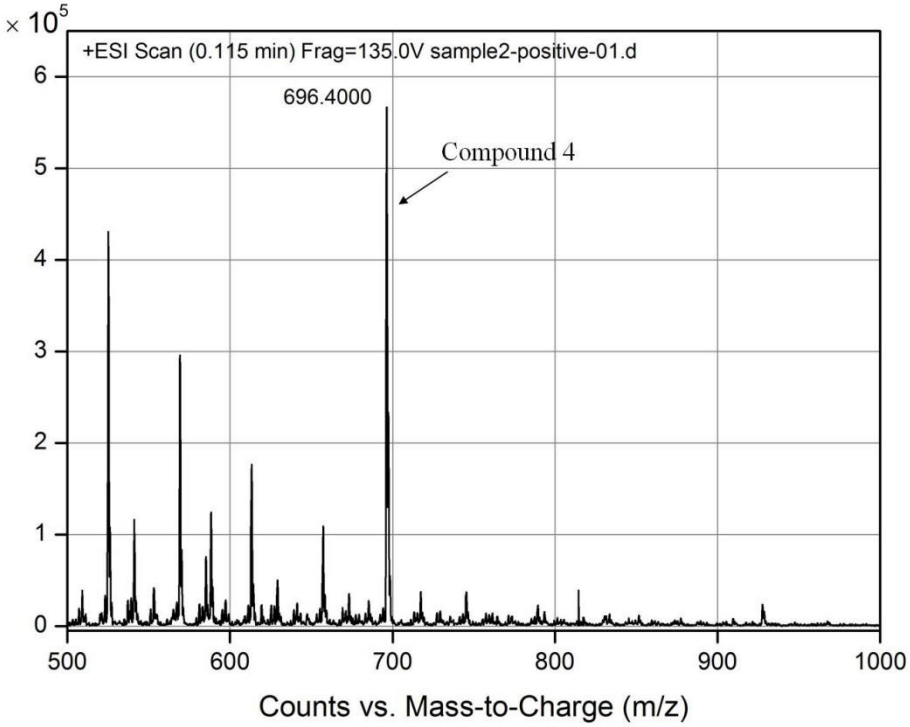

Fig. S11. ESI-MS spectrum of compound 4.

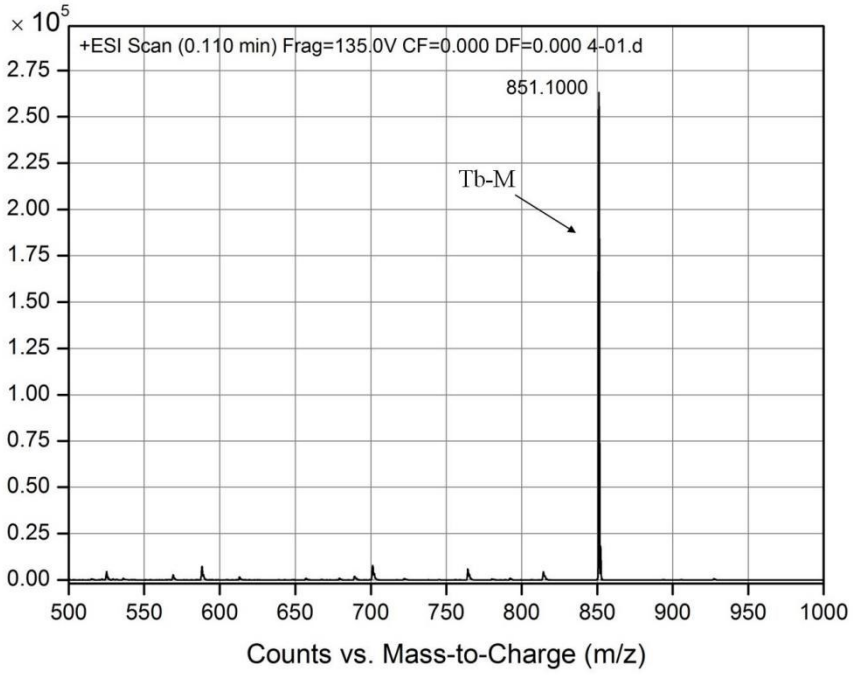

Fig. S12. ESI-MS spectrum of Tb-M.

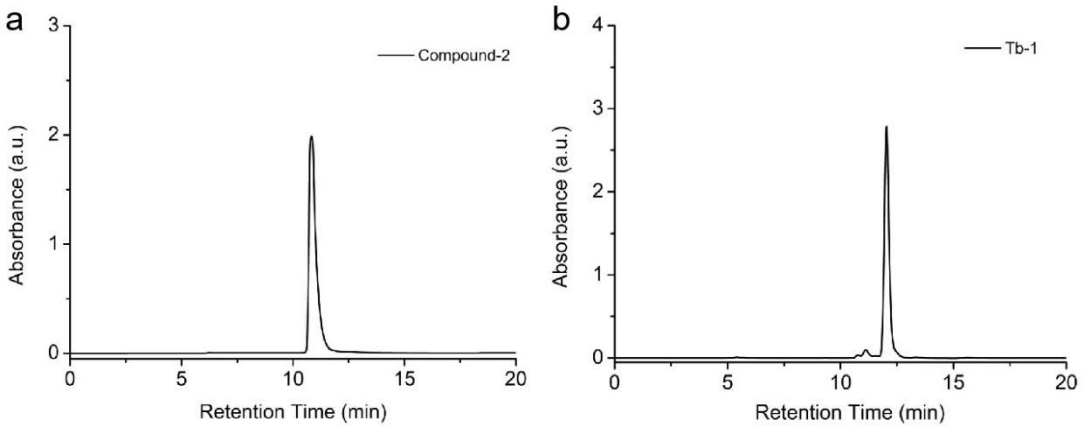

Fig. S13. High-performance liquid chromatography (HPLC) of (a) the compound 2 and (b) Tb-1.

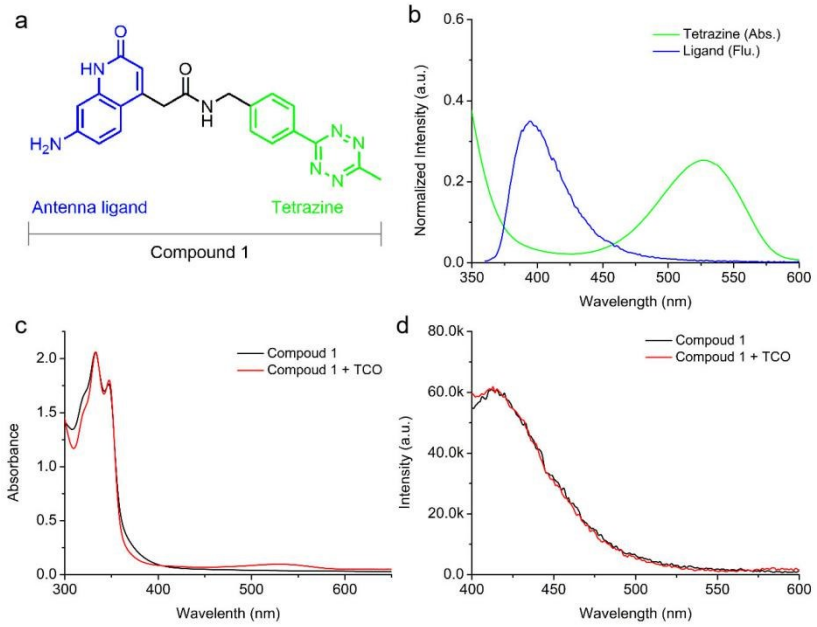

Fig. S14. (a) The chemical structure of compound 1. (b) Absorbance spectra of tetrazine (Abs., green line) together with the fluorescence spectrum of antenna ligand (Flu., blue line). (c) Absorbance and (d) fluorescence spectra of compound 1 in the absence (black line) or presence (red line) of TCO, λ_{ex} = 340 nm.

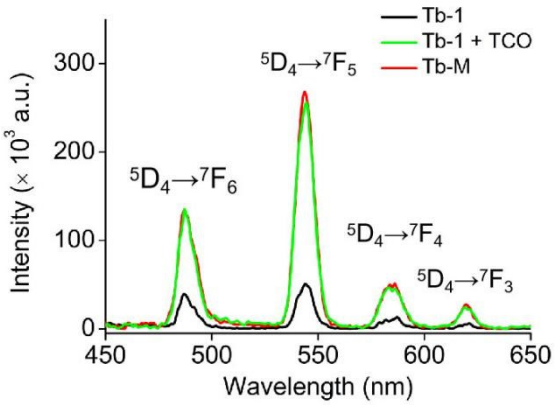

Fig. S15. Luminescence spectra of Tb-M, Tb-1 and its corresponding compound reacted with trans-cyclooctenol (TCO, HEPES pH 7.4); λ_{ex} = 340 nm.

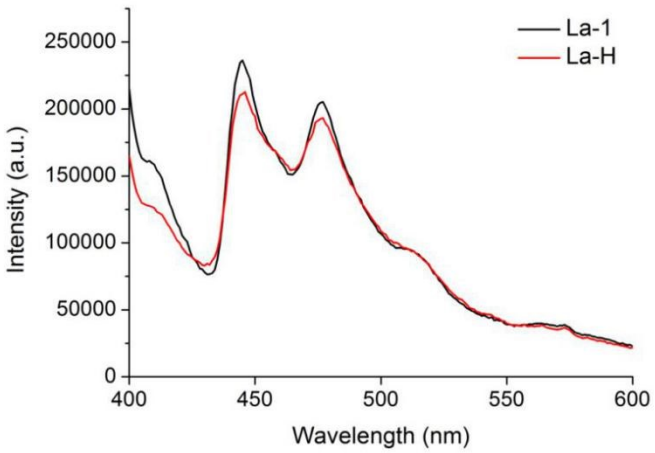

Fig. S16. Normalized emission spectra of La-1 and La-H in H_2O at 77 K.

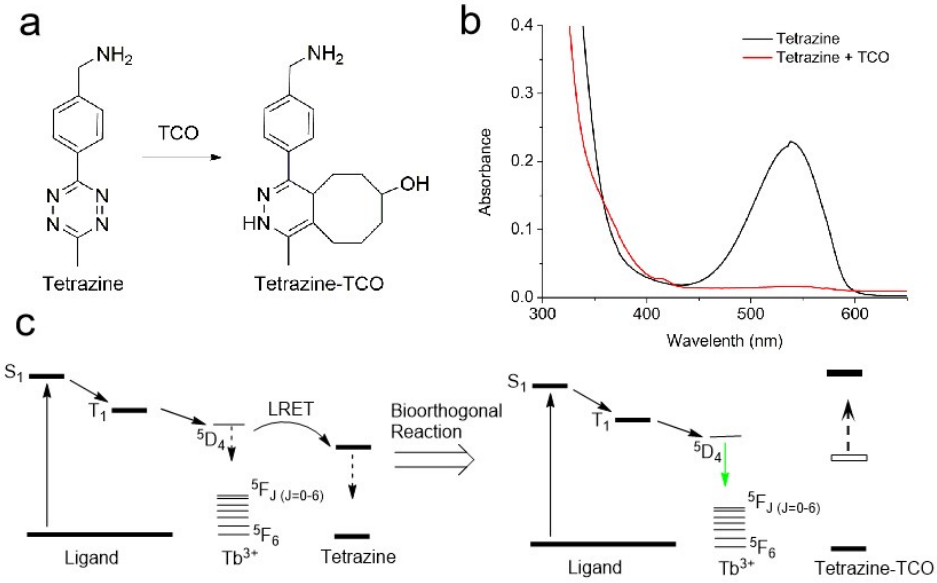

Fig. S17. (a) Schematic illustration of the reaction between tetrazine and TCO. (b) Absorbance spectra of tetrazine in the absence (black line) and presence (red line) of TCO. (c) Proposed energy transfer mechanisms of sensitized terbium emission of Tb-1 and bioorthogonal reaction with TCO.

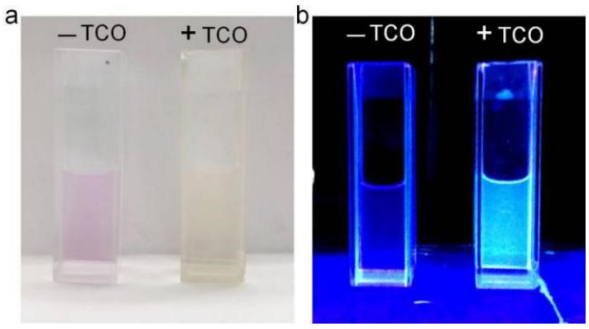

Fig. S18. The photographs of Tb-1 in the absence or presence of TCO (left: bright light; right: λ_{ex} = 340 nm).

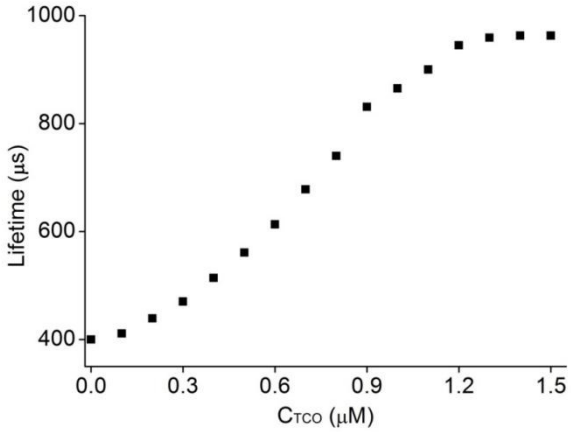

Fig. S19. The relationship between the decay lifetime constant of the $^5D_4 \rightarrow {}^7F_5$ emission of Tb^{3+} and increasing TCO concentration.

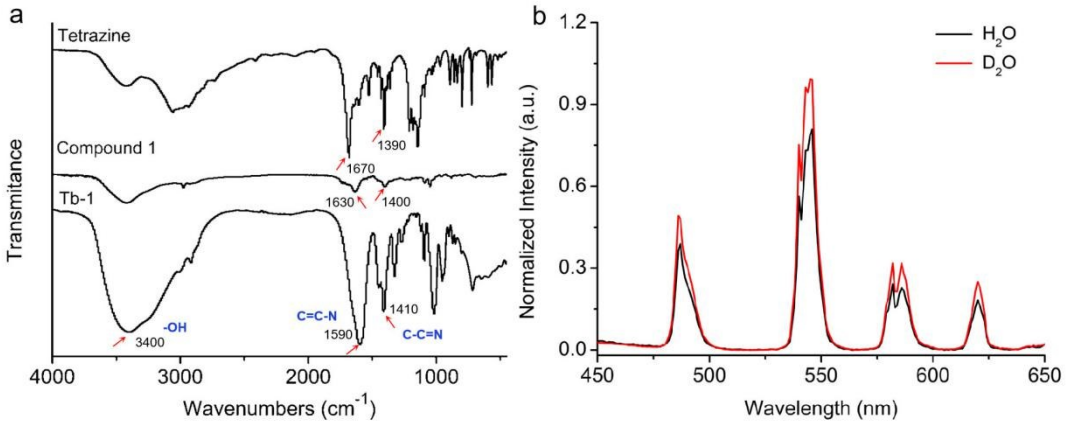

Fig. S20. (a) Fourier transform infrared (FTIR) spectra of the tetrazine, compund 1 and Tb-1. (b) The luminescence of Tb-1 in water (H_2O, black line) or (D_2O, red line), λ_{ex} = 340 nm.

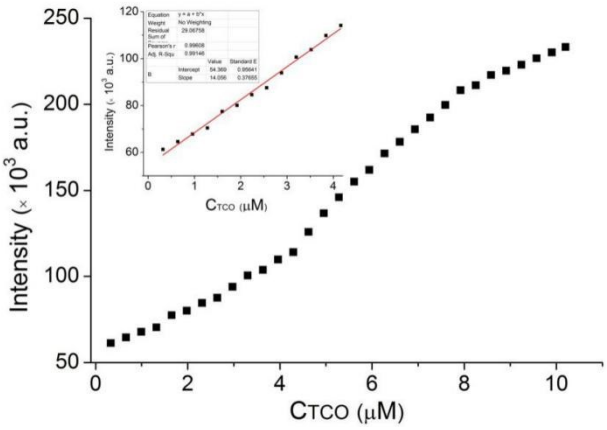

Fig. S21. The luminescence emissions at 545 nm as a function of TCO concentration.

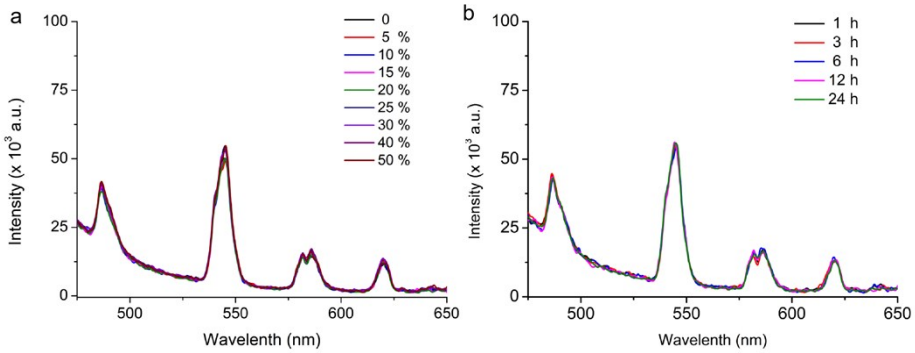

Fig. S22. Changes in luminescence of Tb-1 in PBS buffer solution (pH = 7.4) with (a) different serum concentration (from 0 to 50%), (b) keeping for various time (from 1 to 24 h) in PBS buffer solution (pH = 7.4).

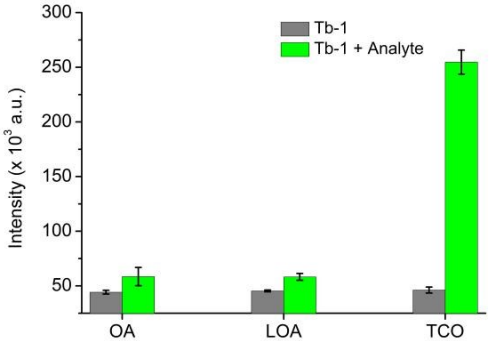

Fig. S23. The changes of luminescence intensity at 545 nm of Tb-1 towards TCO or other unsaturated fatty acids including oleic acid (OA) or linoleic acid (LOA).

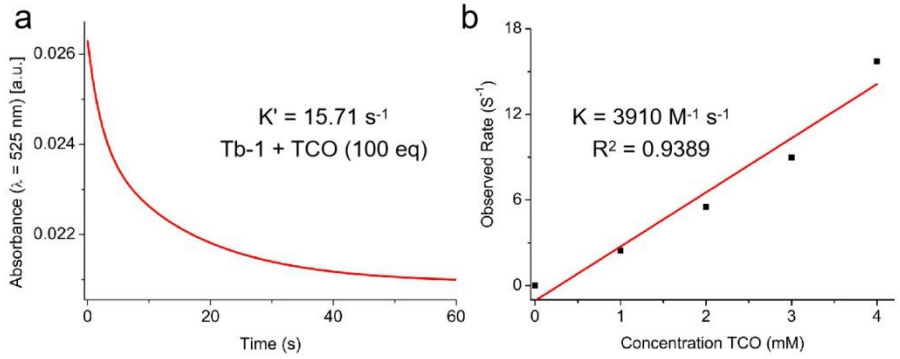

Fig. S24. Characterization of kinetics of the reaction between Tb-1 and TCO by UV-vis spectroscopy. (a) Absorbance at 525 nm of Tb-1 upon TCO addition (100 eq = 4 mM) by fitting the data to the sum of two single exponential equations, observed rates k' values for the fast single exponential equations were determined. (b) Determination of the pseudo-first order rate constant K for the reaction of Tb-1 and TCO.

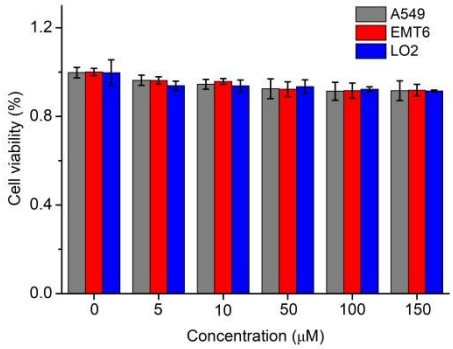

Fig. S25. *In vitro* cell viability of A549, EMT 6 and LO2 cells incubated with different concentration Tb-1.

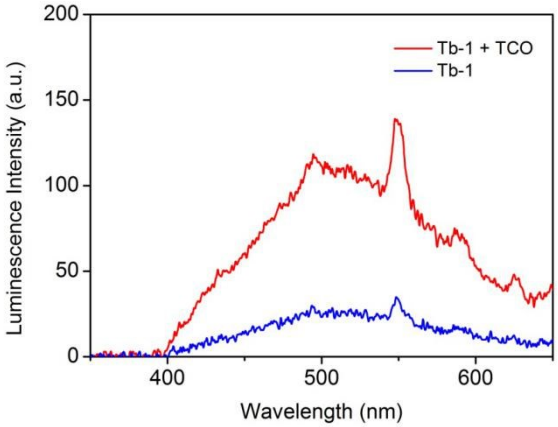

Fig. S26. Two-photo luminescence of Tb-1 with TCO at 298K (λ_{ex} = 730 nm).

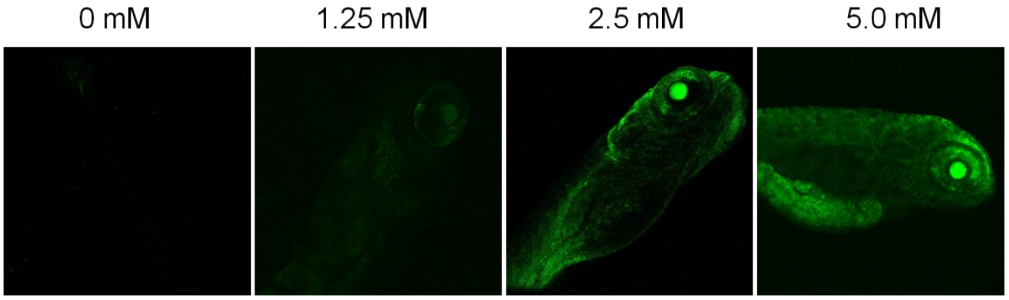

Fig. S27. Dose-dependent generation of TCO groups on the zebrafish after treatment of varied concentration of Ac_4ManNTCO (0, 1.25, 2.5 and 5.0 mM Ac_4ManNTCO in media).

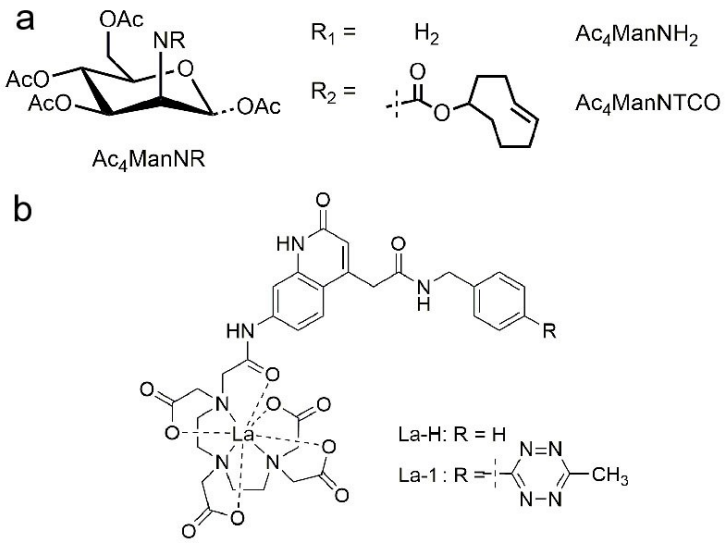

Fig. S28. The chemical structures of (a) Ac_4ManNH_2 and $Ac_4ManNTCO$, and (b) La-H and La-1.